J. Phys. B: At. Mol. Opt. Phys. **33** (2000) 291–302. Printed in the UK PII: S0953-4075(00)02765-6

Rydberg states of the hydrogen atom in the instantaneous van der Waals potential: quantum mechanical, classical and semiclassical treatment

J P Salas† and N S Simonović‡

† Area de Física Aplicada, Universidad de La Rioja, Edificio Politécnico, C/ Luis de Ulloa 20, 26004 Logroño, Spain
‡ Institute of Physics, PO Box 57, 11001 Belgrade, Yugoslavia

Received 17 March 1999, in final form 10 November 1999

Abstract. We present a quantum mechanical, classical and semiclassical study of the energy spectrum of a Rydberg hydrogen atom in the instantaneous van der Waals potential for the $L_z = 0$ case. The semiclassical results are in good agreement with the results of the quantum mechanical calculations within the first-order perturbation theory as well as with the quantum mechanical calculations of other authors. The classical analysis shows that the phase space of the system is separated into the regions of vibrational and rotational motions, which are connected, respectively, with the lower-lying energy levels of doublet symmetry, and with the non-degenerate higher-energy levels. Finally, we compare the classical (eigen)trajectories with the corresponding eigenstates and find that both of them show the same symmetry patterns.

1. Introduction

The term van der Waals interaction is generally reserved for attractive forces between neutral bodies, where the electric dipole momenta are primarily responsible for this interaction. Originally, this interaction was introduced in order to explain an attractive potential between molecules of a gas, which is proportional to R^{-6}, where R is the distance between two molecules. Moreover, the term is also used for the Lennard-Jones dipole attraction between an atom and its image in a planar conducting surface, for which the potential varies with d^{-3}, where d is the atom–surface distance. The applicability of the electrostatic image model to this case has been discussed in several papers (see e.g. Lennard-Jones 1932, Zaremba and Kohn 1976, Fabre *et al* 1983) and has also been verified experimentally (Fabre *et al* 1983, Anderson *et al* 1988, Sandoghder *et al* 1992). In particular, for highly excited Rydberg atoms, the outer electron has a very low characteristic frequency compared with the frequencies of the electrons in a metal. Hence, the calculation of the atom–metal potential can be performed using an adiabatic approximation where it is supposed that the metal electrons adjust themselves to the instantaneous position of the atomic electron. This interaction is usually called *the instantaneous van der Waals interaction*.

In this study, we consider the problem of a Rydberg hydrogen atom at a large distance from a metal surface (i.e. for $d \gg r$, where r is the electron–nucleus distance) under the approximation of the instantaneous van der Waals interaction. The corresponding potential can be obtained as the quadratic approximation of the exact atom–surface potential (Ganesan

0953-4075/00/030291+12$30.00

and Taylor 1996). Using cylindrical coordinates (ρ, z, φ) and atomic units, the Hamiltonian of the system takes the form

$$\mathcal{H} = \frac{p^2}{2} - \frac{1}{r} - \frac{1}{16d^3}(r^2 + z^2), \tag{1}$$

where $r = (\rho^2 + z^2)^{1/2}$, $p^2 = p_\rho^2 + L_z^2/\rho^2 + p_z^2$ and d is the nucleus–surface distance. Due to the cylindrical symmetry of the problem, the z-component of the angular momentum L_z is conserved and the φ-motion is separated from that in the (ρ, z) plane. Within the framework of classical mechanics, Hamiltonian (1) represents a non-integrable two-dimensional dynamical system. Here we consider the $L_z = 0$ case.

The instantaneous van der Waals interaction corresponds to the special case $\beta = \sqrt{2}$ of the generalized van der Waals interaction $V \sim r^2 + (\beta^2 - 1)z^2$ introduced by Alhassid *et al* (1987). For Rydberg atoms weakly perturbed by this potential, these authors showed that an adiabatic invariant Λ exists for all particular values of β. Moreover, Λ is a generalization of the corresponding invariant found by Solov'ev (1982) for the quadratic Zeeman effect ($\beta = 0$). In the case of the instantaneous van der Waals interaction, this adiabatic invariant has the form

$$\Lambda = 2\boldsymbol{A}^2 + 5A_z^2, \tag{2}$$

where A_z is the z-component of the Runge–Lenz vector $\boldsymbol{A}$. Semiclassical quantization of the hydrogen atom in the generalized van der Waals interaction was performed for a few (integrable) cases by Ganesan and Lakshmanan (1992), and also for the hydrogen atom in a strong magnetic field—the quadratic Zeeman effect—(Delos *et al* 1983, Farrelly and Krantzman 1991) and in parallel electric and magnetic fields (Waterland *et al* 1987). However, the special case of the instantaneous van der Waals interaction was not considered in any detail. In this paper we carry out the analysis of this problem using similar techniques to those of the above-mentioned cases.

The paper is organized as follows. In section 2, we calculate the Rydberg states of the hydrogen atom in the instantaneous van der Waals interaction within the first-order quantum perturbation theory. In section 3, we consider the problem classically, and we generate, in terms of the Keplerian action-angle variables, an integrable approximation (*normal form*) to the original nonintegrable Hamiltonian. In section 4, we obtain the energy spectrum by semiclassical quantization of the normalized classical motion. In section 5, we compare the classical and quantum dynamics (the so-called eigentrajectories and eigenfunctions). Finally, in section 6, we summarize and discuss the results.

2. Quantum perturbation theory

By taking the last term in Hamiltonian (1) as a perturbation, the effects of the instantaneous van der Waals interaction on the energy spectrum of the hydrogen atom may be calculated by using first-order degenerate perturbation theory. The eigenstates of (1) can be expressed as a function of the pure hydrogenic basis by using the following expansion over the orbital quantum number l:

$$\Psi_{n,k}(r, \vartheta) = \sum_{l=0}^{n-1} c_l^{nk} R_{nl}(r) Y_l^0(\vartheta, 0), \qquad k = 0, \ldots, n-1, \tag{3}$$

since $m = 0$ and n remains a good quantum number within the first-order theory. The values of the c_l^{nk} coefficients follow after solving the secular problem for the perturbation, which involves the diagonalization of a matrix obtained by representing the operator $r^2 + z^2$ in the hydrogenic basis $\{|nlm\rangle; l = 0, \ldots, n-1; m = 0\}$. We note that, because $\mathcal{H}$ commutes

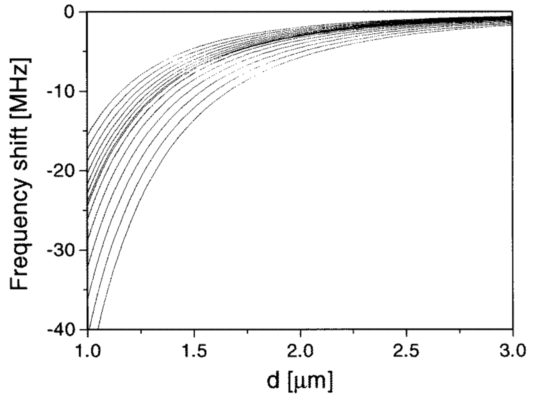

Figure 1. The energy (frequency) level shifts of the $n = 20$ manifold. The lower energy levels have the doublet symmetry and correspond to the vibrational trajectories, while the upper non-degenerated levels correspond to the rotational trajectories.

with the parity operator Π, each eigenstate $\Psi_{n,k}(r, \vartheta)$ has the same definite parity as the corresponding unperturbed eigenstate. The required matrix elements are

$$\begin{aligned}\langle nl0|r^2+z^2|nl'0\rangle = {} & \frac{5n^2}{2}\sqrt{(n^2-l^2)[n^2-(l-1)^2]}\,\frac{l(l-1)}{(2l-1)\sqrt{(2l-3)(2l+1)}}\delta_{l,l'+2} \\ & +\frac{n^2}{2}[5n^2-3l(l+1)+1]\left[1+\frac{2l^2+2l-1}{(2l-1)(2l+3)}\right]\delta_{ll'} \\ & +\frac{5n^2}{2}\sqrt{[n^2-(l+2)^2][n^2-(l+1)^2]}\,\frac{(l+2)(l+1)}{(2l+3)\sqrt{(2l+1)(2l+5)}}\delta_{l,l'-2}.\end{aligned} \tag{4}$$

If we denote the eigenvalues of this matrix by $(r^2+z^2)_{nk}$, the energy shifts are

$$\Delta E_{n,k} = -\frac{1}{16d^3}(r^2+z^2)_{nk}. \tag{5}$$

Thus, the energy levels $E_{n,k} = -1/2n^2 + \Delta E_{n,k}$ are shifted downwards with regard to those of the unperturbed atom.

The values of the energy-level shifts $\Delta E_{n,k}$ (in MHz) for the $n = 20$ manifold in the range of $d = 1$–$3\ \mu$m are shown in figure 1. The unperturbed degeneracy is partially removed in such a way that each n-manifold divides into two parts: *the lower-lying energy levels of doublet symmetry* with the dominant contribution of the lower angular momenta l in the corresponding states, and *the non-degenerate higher-energy levels* where the partial waves with higher angular momenta predominate in the wavefunctions. The results of these calculations are discussed in more detail in sections 4 and 5, where they are compared with the corresponding semiclassical results (the last two columns in tables 2 and 3). We note that these results are in good agreement with those of Alhassid *et al* (1987).

3. Classical perturbation theory

For sufficiently large d, this Rydberg system appears nearly integrable (Simonović 1997), and from the point of view of astronomers, the Hamiltonian (1) represents a perturbed Keplerian system to which the methods of celestial mechanics apply. This is what Uzer *et al* (1991) call ‘celestial mechanics on a microscopic scale’. A normalization in the usual sense (Abraham and Marsden1980) allows us to reduce the problem to an integrable dynamical system where only one degree of freedom is left. To carry out the reduction, a Lie transformation (Deprit 1969) is sufficient. From the reduction, the new Hamiltonian admits the principal action (corresponding to the principal quantum number n) as an integral. As performed by Coffey *et al* (1986) for the Zeeman effect, Deprit *et al* (1996) for the Stark–Zeeman effect and Elipe and Ferrer (1994) for the generalized van der Waals potential, we perform the normalization in the Delaunay variables (Goldstein 1980) $(I_1, I_2, I_3, \phi_1, \phi_2, \phi_3)$, which are the Keplerian action-angle variables. The Delaunay normalization (Deprit 1981) is a canonical transformation

$$(I_1, I_2, I_3, \phi_1, \phi_2, \phi_3) \longrightarrow (I_1', I_2', I_3', \phi_1', \phi_2', \phi_3')$$

which converts $\mathcal{H}$ into a function that does not depend on the averaged mean anomaly ϕ_3'. By performing the reduction to the first order, and after dropping the primes in the new variables, the normalized Hamiltonian (for the special case $I_1 = L_z = 0$) comes out as the sum

$$\begin{aligned} \mathcal{H}' &= \mathcal{H}_0' + \mathcal{H}_1' \\ \mathcal{H}_0'(\phi_2, I_2) &= -\frac{1}{2I_3^2}, \\ \mathcal{H}_1'(\phi_2, I_2) &= -\frac{I_3^4}{64d^3}\left[6 + 9\left(1 - \frac{I_2^2}{I_3^2}\right) - 5\left(1 - \frac{I_2^2}{I_3^2}\right)\cos 2\phi_2\right], \end{aligned} \tag{6}$$

where I_3 is the principal Delaunay action, corresponding to the principal quantum number n, I_2 is the angular momentum corresponding to the quantum number l, and ϕ_2 is the argument of the perinucleus (the angle between the Runge–Lenz vector and the nodal line). As a consequence of $I_1 = 0$, the angular momentum I_2 remains in the (x, y) plane and ϕ_2 is the angle between the Runge–Lenz vector and the ρ-axis. The algebraic manipulations were executed with the symbolic processor MATHEMATICA (Wolfram 1996). Since I_3 is a constant of motion, the integral $\mathcal{H}_0'$ may be neglected, and the normalized Hamiltonian reduces to $\mathcal{H}_1'$. The (one-dimensional) phase portrait of $\mathcal{H}_1'$ is shown in figure 2(*a*). As we can observe in this figure, the phase space has the structure of a twofold hindered rotor (Farrelly and Krantzman 1991): a separatrix passing through the two hyperbolic equilibria located at $(\pi, 0)$ and $(0, 0)$ forms two symmetric homoclinic loops surrounding the elliptic equilibria located at $(\pi/2, 0)$ and $(3\pi/2, 0)$. It is worthwhile noting that the maps of $\mathcal{H}'$ on the cylinders (ϕ_2, I_2) do not cover the entire phase space, because they exclude the circular orbits ($I_2 = I_3$). This singularity disappears (Deprit and Ferrer 1990) when the system is treated with the following variables:

$$u = e\cos\phi_2, \qquad v = e\sin\phi_2, \qquad w = \pm\sqrt{1 - e^2} = \pm\frac{I_2}{I_3}, \tag{7}$$

where $e = \sqrt{1 - I_2^2/I_3^2}$ is the eccentricity of the electronic orbits. It is worth noting that (u, v) are the Cartesian components of the Runge–Lenz vector ($u^2 + v^2 = \boldsymbol{A}^2$, $v = A_z$), while w is the norm of the angular momentum I_2 divided by I_3. In this new map (u, v, w), given that

$$u^2 + v^2 + w^2 = 1,$$

the phase space consists of a unit-radius sphere. In these coordinates, the points with $w > 0$ ($I_2 > 0$) stand for Keplerian ellipses travelled in a direct (prograde) sense, while those points with $w < 0$ ($I_2 < 0$) represent Keplerian ellipses travelled in a retrograde sense. Moreover, any point in the equatorial circle $w = 0$ ($I_2 = 0$) corresponds to a straight line passing through the origin. Finally, the north (south) pole corresponds to circular orbits ($e = 0$) travelled in a direct (retrograde) sense. In coordinates (u, v, w) the Hamiltonian $\mathcal{H}_1'$ becomes the function

$$\mathcal{H}_1' = -\frac{I_3^4}{32d^3}[3 + 2u^2 + 7v^2]. \tag{8}$$

Note at this point, that $2u^2 + 7v^2$ is none other than the adiabatic invariant (2) (see below equations (12)). The corresponding phase space is shown in figure 2(*b*). The Hamiltonian (8)

Table 1. The stability, energy and type of orbit of the equilibria.

Equilibrium	Stability	Energy	Type of orbit
$E_{1,2} = (\pm 1, 0, 0)$	Unstable	$\mathcal{E}_{1,2} = -5I_3^4/32d^3$	Linear along the ρ-axis
$E_3 = (0, 1, 0)$	Stable	$\mathcal{E}_3 = -5I_3^4/16d^3$	Linear along the $z \leqslant 0$-axis
$E_4 = (0, -1, 0)$	Stable	$\mathcal{E}_4 = -5I_3^4/16d^3$	Linear along the $z \geqslant 0$-axis
$E_{5,6} = (0, 0, \pm 1)$	Stable	$\mathcal{E}_{5,6} = -3I_3^4/32d^3$	Circular

indicates that the phase flow is time-reversal symmetric with respect to the planes $u = 0$, $v = 0$ and $w = 0$. Consequently, the equilibria, if any, must lie on $(\pm 1, 0, 0)$, and/or on $(0, \pm 1, 0)$ and/or on $(0, 0, \pm 1)$. In this way, taking into account the Jacobi–Liouville theorem and the Poisson brackets between the variables (u, v, w)

$$[u, v] = w, \qquad [v, w] = u, \qquad [w, u] = v,$$

the equations of motion associated with $\mathcal{H}_1'$ are

$$\begin{aligned}\dot{u} &= [u, \mathcal{H}_1'] = -\frac{7I_3^4}{16d^3}vw,\\ \dot{v} &= [v, \mathcal{H}_1'] = \frac{I_3^4}{8d^3}uw,\\ \dot{w} &= [w, \mathcal{H}_1'] = \frac{5I_3^4}{16d^3}uv.\end{aligned} \tag{9}$$

Equating the right-hand members of equations (9) to zero, we arrive at the six equilibria appearing in table 1. This table also shows the corresponding stability, energy and type of orbit. We performed the stability analysis by studying the roots of the characteristic equation resulting from the variational equations of motion (Coffey *et al* 1986, Salas *et al* 1998). The equilibria E_1 and E_2 presented in figure 2(*b*) are the equilibria located at $(0(2\pi), 0)$ and $(\pi, 0)$; while E_2 and E_3 are the equilibria located at $(\pi/2, 0)$ and $(3\pi/2, 0)$. Finally, the contour lines $I_2 = \pm I_3$ are represented by the equilibria E_5 and E_6, respectively.

In figures 2(*a*) and (*b*), we observe four families of contour lines. The two families of levels V_1 (V_2) around the equilibria E_3 (E_4) correspond to quasiperiodic orbits oscillating around the linear orbits E_3 (E_4) (see figure 2(*d*)). This kind of motion belongs to the so-called *vibrational* motion (Wintgen and Friedrich 1989). The two families of phase trajectories R around the equilibria $E_{5,6}$ correspond to quasiperiodic orbits oscillating around the circular orbits E_5 (E_6) (see figure 2(*c*)). This motion is usually named as *rotational* motion (Wintgen and Friedrich 1989). We note that the rotational levels around $E_{5,6}$ are equivalent because they represent the same orbits travelled in either the direct (around E_5) or retrograde sense (around E_6). However, vibrational levels V_1 and V_2 represent different orbits, although they have the same energy. For plotting the figures 2(*c*) and (*d*), we used the (x', y') orbital plane, which in the case of $I_1 = 0$ maps to the (ρ, z) plane by the transformations $\rho = |x'|$, $z = y'$.

For the problem of a Rydberg hydrogen atom in strong magnetic and electric fields, an explanation has been given on how similar families of rotators and librators are connected to the quantum states of the system (Delos *et al* 1983, Cacciani *et al* 1986). In this way, each classical phase space trajectory with an appropriately quantized value of the action variable corresponds to a quantum state. Hence, those quantum states corresponding to vibrational states are degenerate and have lower energies; those corresponding to rotational states are nondegenarate and have higher energies. We note that this is the information about the level structure which is difficult to obtain from quantum mechanics.

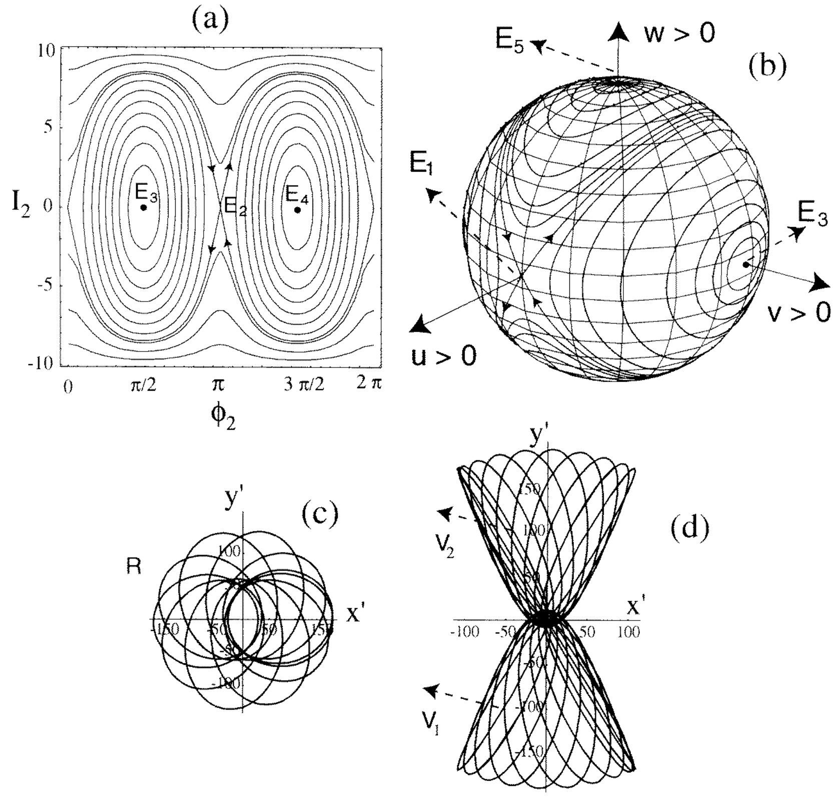

Figure 2. (*a*) The phase portrait (ϕ_2, I_2) at various values of $d^3\mathcal{H}'_1$, for $I_3 = n = 10$ and $I_1 = m = 0$. (*b*) The phase portrait on the sphere for the same parameters. (*c*) Characteristic rotational level. (*d*) Typical vibrational levels V_1 and V_2.

4. Semiclassical quantization

From the semiclassical point of view, each regular trajectory having appropriately quantized values of the action variables (i.e. which satisfy the EBK quatization rules) corresponds to a quantum state. Such trajectories are usually called the *eigentrajectories*. More exactly, the whole class of the trajectories confined on an invariant torus determined by quantized values of the action variables is that which corresponds to a quantum state (Berry 1983). However, we can take an arbitrary trajectory on the torus as representative. Since the system determined by the normal form (6) is integrable, it can be quantized by applying the EBK rules (Gallagher 1994) to the action variables (I_1, I_2, I_3). Here I_1 and I_3 are exact and approximate constants of motion, respectively, and they can be quantized as in the unperturbed Kepler problem (Waterland *et al* 1987)

$$I_1 = m, \qquad I_3 = n, \tag{10}$$

where m and n are the magnetic and the principal quantum numbers, respectively. However, because of the presence of the instantaneous van der Waals interaction, the angular momentum I_2 is not a constant of motion, and the action which has to be quantized for the perturbed problem is the following (Waterland *et al* 1987):

$$A = \frac{1}{2\pi} \oint_C I_2 \,\mathrm{d}\phi_2 = k + \tfrac{1}{2}. \tag{11}$$

For a vibrational trajectory, A is $1/2\pi$ times the area enclosed by loop C, while for a rotational trajectory, it is $1/2\pi$ times the area between the rotator line and the $I_2 = 0$ line (see figure 2(a)). We saw in the previous section that $2u^2 + 7v^2$, which contributes to $\mathcal{H}'_1$ in (8), is in fact the adiabatic invariant Λ given by (2). Thus, we can write $\mathcal{H}'_1$ in the form

$$\begin{aligned} \mathcal{H}'_1 &= -\frac{I_3^4}{32d^3}(3 + \Lambda(\phi_2, I_2; I_3)), \\ \Lambda &= \frac{9}{2}\left(1 - \frac{I_2^2}{I_3^2}\right) - \frac{5}{2}\left(1 - \frac{I_2^2}{I_3^2}\right)\cos 2\phi_2. \end{aligned} \tag{12}$$

It is clear that Λ is an (approximate) constant of motion (because $\mathcal{H}'_1$ and I_3 are), which takes the values $0 < \Lambda < 7$ ($\Lambda = 2$ for the separatrix). In order to quantize Hamiltonian (12), we express Λ in terms of variables A and I_3 rather than in terms of I_3, I_2 and ϕ_2. After solving equation (12) for action I_2, the action integrals A for the rotational and vibrational motions give

$$\begin{aligned} A_{\mathrm{rot}} &= \frac{1}{2\pi}\int_0^{2\pi} I_2\,\mathrm{d}\phi_2 = \frac{I_3}{2\pi}\int_0^{2\pi}\sqrt{1 - \frac{2\Lambda}{9 - 5\cos 2\phi_2}}\,\mathrm{d}\phi_2, \qquad 0 < \Lambda < 2, \\ A_{\mathrm{vib}} &= \frac{1}{2\pi}\int_{\phi_2^0}^{\pi-\phi_2^0} I_2\,\mathrm{d}\phi_2 = \frac{I_3}{2\pi}\int_{\phi_2^0}^{\pi-\phi_2^0}\sqrt{1 - \frac{2\Lambda}{9 - 5\cos 2\phi_2}}\,\mathrm{d}\phi_2, \qquad 2 < \Lambda < 7, \end{aligned} \tag{13}$$

where $\phi_2^0 = \frac{1}{2}\arccos((9 - 2\Lambda)/5)$.

Then, in order to obtain Λ for any given quantized values $A = k + \frac{1}{2}$ and $I_3 = n$ (rules (10), (11)), we have to solve the following equation:

$$\mathcal{J}(\Lambda) = 2\pi\frac{k + \frac{1}{2}}{n}, \tag{14}$$

where $\mathcal{J}(\Lambda)$ are the integrals appearing in (13). This can be done by using an appropriate numerical procedure for finding zeros, combined with numerical integration of $\mathcal{J}(\Lambda)$. The domains of the function $\Lambda = \mathcal{J}^{-1}(2\pi A/I_3)$ for the vibrational and rotational cases are: (V) $0 < A/I_3 < 0.320\,491$, (R) $0.640\,983 < A/I_3 < 1$. If we label the solution of equation (14) with $\Lambda_{n,k}$, we get the following semiclassical energy formula:

$$E_{n,k} = -\frac{1}{2n^2} - \frac{n^4}{32d^3}(3 + \Lambda_{n,k}). \tag{15}$$

Since $0 < \Lambda_{\mathrm{rot}} < 2 < \Lambda_{\mathrm{vib}} < 7$, each n-manifold divides into two separate parts, the lower-lying vibrational levels and the higher rotational levels. The domains of the variable $A/I_3 = (k + \frac{1}{2})/n$ for the vibrational and rotational motions determine the allowed values for the semiclassical quantum number k:

$$\begin{aligned} &k = 0, \ldots, [0.320\,491n - 0.5] && \text{for vibrational levels,} \\ &k = [0.640\,983n + 0.5], \ldots, n - 1 && \text{for rotational levels,} \end{aligned} \tag{16}$$

where $[a]$ denotes the integer value of a. For example, if $n = 10$, $[a]$ is $k = 0, 1, 2$ for vibrational and $k = 6, 7, 8, 9$ for rotational levels. When we take into account that the vibrational levels are doubly degenerate, it follows that the $n = 10$ manifold consists exactly of ten different semiclassical states, as expected (see table 2).

The results of the calculations for $n = 10$ at $d = 100$ nm and $n = 20$ at $d = 1$ μm are shown in tables 2 and 3, together with the results of the quantum mechanical calculations from section 2. It can be seen that the semiclassical results are in good agreement with the quantum mechanical. (The plot of semiclassical energy levels for $n = 20$ in the range $d = 1$–3 μm practically coincides with figure 1.) The tiny splitting of the degeneracy appearing for

Table 2. The energy-level shifts of the $n = 10$ manifold at $d = 100$ nm (in GHz)—semiclassical and quantum mechnical results. k is the semiclassical quantum number. The corresponding types of the classical motions can be (doubly degenerate) vibrational (V_1, V_2) and rotational (R). The parity (even/odd) of the quantum mechanical states is also presented.

k	Classical type	Semiclassical results	Quantum results	Parity
			−2.7173	e
0	V_1, V_2	−2.7051	−2.7173	o
			−2.1437	e
1	V_1, V_2	−2.1313	−2.1437	o
			−1.7262	e
2	V_1, V_2	−1.7101	−1.7209	o
6	R	−1.5168	−1.5051	e
7	R	−1.3920	−1.4047	o
8	R	−1.2243	−1.2325	e
9	R	−1.0248	−1.0335	o

Table 3. The energy-level shifts of the $n = 20$ manifold at $d = 100$ μm (in MHz)—semiclassical and quantum mechanical results. k is the semiclassical quantum number. The corresponding types of the classical motions can be (doubly degenerate) vibrational (V_1, V_2), rotational (R) or rovibrational which lies close to the separatrix (S). The parity (even/odd) of the quantum mechanical states is also presented.

k	Classical type	Semiclassical results	Quantum results	Parity
0	V_1, V_2	−45.9462	−45.9950 −45.9950	e o
1	V_1, V_2	−40.7639	−40.8129 −40.8129	e o
2	V_1, V_2	−36.1727	−36.2220 −36.2220	e o
3	V_1, V_2	−32.1809	−32.2309 −32.2309	e o
4	V_1, V_2	−28.8059	−28.8578 −28.8576	e o
5	V_1, V_2	−26.0928	−26.1628 −26.1399	e o
12	S	−24.3788	−24.4655	e
13	R	−23.8632	−23.9748	o
14	R	−22.8503	−22.8625	e
15	R	−21.6543	−21.6875	o
16	R	−20.3106	−20.3443	e
17	R	−18.8355	−18.8701	o
18	R	−17.2384	−17.2733	e
19	R	−15.5257	−15.5607	o

the quantum mechanical values of the vibrational energy levels near the classical separatrix is due to a tunnelling between vibrational states V_1 and V_2 in the vicinity of the separatrix. This splitting does not appear in the semiclassical energy levels because the EBK rules do not incorporate tunnelling effects.

In some cases (e.g. for $n = 20$, table 3) formula (16) gives $n - 1$ instead of n levels for a given manifold. The comparison with the quantum mechanical calculations indicates that the ‘missing’ state (i.e. eigentrajectory) lies in the close neighbourhood of the separatrix. This effect appears because the states near the separatrix are subjected to quantum mechanical tunnelling (Waterland *et al* 1987), and the semiclassical theory applied here does not take this into account. Therefore, within this approach we cannot exactly find and categorize the missing semiclassical state. However, since the missing state is a singlet, the corresponding energy level is non-degenerate; it can therefore be estimated by using the following *ad hoc* rule in the neighbourhood of the separatrix:

$$A_{\mathrm{rot}} = k^* + \tfrac{1}{2}, \qquad k^* = [0.640\,983n + 0.5] - 1. \tag{17}$$

In practice, this involves the calculation of an additional rotational level with $k = k^*$, although in this case A/I_3 goes slightly out of the domain. Alternatively, the energy of the missing state can be roughly estimated by simply taking $\Lambda = 2$, which in fact gives the energy of the motion on the separatrix

$$E_{n,k^*} \approx E_n^{\mathrm{sep}} = -\frac{1}{2n^2} - \frac{5n^4}{32d^3}. \tag{18}$$

Apart from the case of a missing state, there are cases in which by using formula (16) there appear $n+1$ states in a given n-manifold (e.g. for $n = 11$). The comparison with the quantum mechanical calculations indicates that in this case, the highest vibrational (doublet) energy level should in fact be the lowest rotational (non-degenerate) level. Here, we are also dealing with a state which lies close to the separatix and, as mentioned above, we cannot exactly evaluate and determine the type of such a state within the semiclassical approach; although its energy can be estimated by using (17) or (18).

5. Eigenfunctions and eigentrajectories

The next step is to study, for a given n-manifold, the new pattern imposed by the van der Waals interaction on the eigenstates and eigentrajectories structure. The eigenfunctions are calculated by using expansion (3) with the coefficients c_l^{nk}, which are the components of the eigenvectors of the secular matrix (4). The corresponding eigentrajectories are calculated by taking arbitrary initial conditions in the appropriate quantized phase curve (ϕ_2, I_2). Once again, we use the (x', y') orbital plane for all these plots. A set of eigentrajectories and eigenfunctions for $n = 10$ at $d = 100$ nm is shown in figure 3. Each eigenfunction (right column) is associated with its corresponding eigentrajectory (left column) labelled with the semiclassical quantum number k and with the type of classical motion $V_{1,2}$ or R (see table 2). From this figure, we observe that in all cases the wavefunction seems to follow the 'tracks' of the eigentrajectory, because the wavefunction is mainly localized inside the region of the orbital plane occupied by the eigentrajectory. For vibrators (figure 3(*a*)), the wavefunctions are mainly localized along the z (y') direction (figure 3(*b*)). This inspection reveals a principal difference between the quantum mechanical and the semiclassical pictures for these states: in the quantum mechanical treatment the even/odd wavefunctions are in fact linear combinations of two degenerate vibrational states corresponding to V_1 and V_2 classical configurations, and the degeneracy is split at the higher order because of tunnelling between them, whereas in the semiclassical approach, these configurations are quantized separately, giving exact doubly degenerate levels (without tiny splitting). For rotators (figure 3(*c*)), the wavefunctions of both even and odd parties are symmetrically distributed around the origin in the orbital plane (figure 3(*d*)).

6. Concluding remarks

In order to obtain an overall view of the results of this work, we pay attention to the following points. (i) We have presented a combined quantum, classical and semiclassical study of

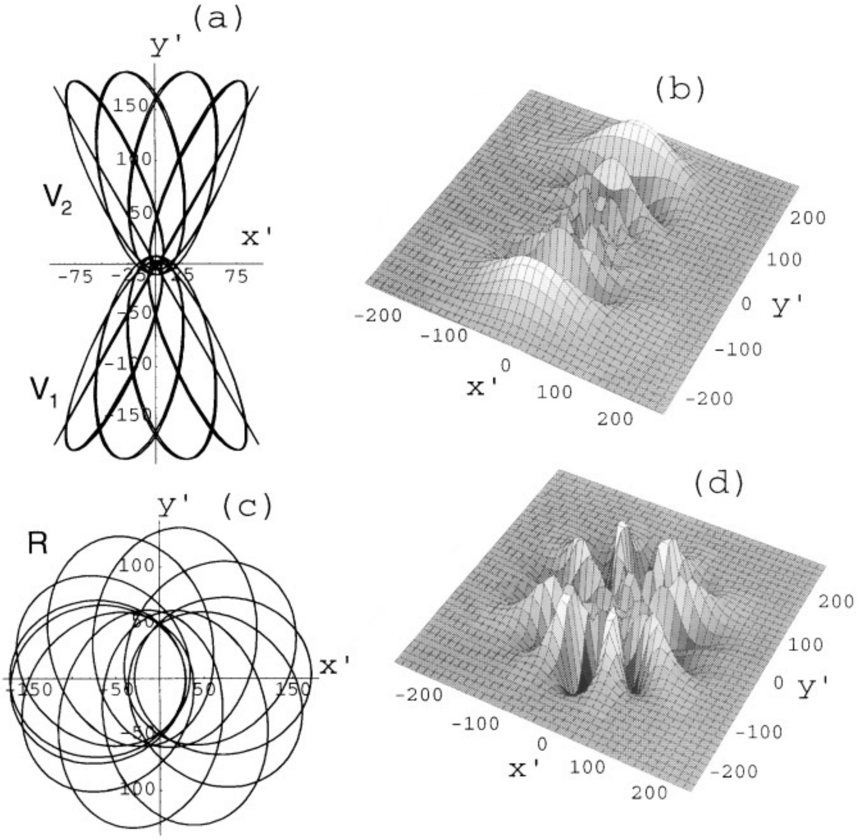

Figure 3. (*a*) and (*c*) show the vibrational (V_1, V_2) and rotational (R) eigentrajectories for $n = 10$ and $m = 0$ ($k = 0$ and 9, respectively), whereas (*b*) and (*d*) correspond to the first-order perturbed eigenstates for the same parameters.

the problem. (ii) The EBK semiclassical results are in good agreement with the quantum mechanical results (see tables 2 and 3), which are also in good agreement with the quantum mechanical calculations of Ganesan and Taylor (1996) as well as with the spectroscopic measurements of the energy of interaction between Rydberg atoms (10–13 S states of sodium) and its images in the walls of a micrometre-sized cavity (Sandoghder *et al* 1992). (iii) By means of the contour plots of the normalized Hamiltonian $\mathcal{H}_1'$ (both in variables (I_2, ϕ_2) and (u, v, w)), we have found that the classical and the quantum states are sorted into two different families: the vibrational and the rotational states. (iv) In the quantum mechanical calculations, a tiny splitting of the degeneracy appearing in the vibrational levels near the classical separatrix results from tunnelling between vibrational states in the vicinity, but from different sides of the separatrix. This splitting does not appear in the semiclassical results because EBK quantization rules do not incorporate tunnelling effects. (v) On comparing vibrational (rotational) eigentrajectories to vibrational (rotational) eigenstates, we have found that both cases show the same symmetry patterns. (vi) We point out that classical mechanics proves to be a powerful tool which provides a compact geometric picture of the energy-level structure of the perturbed Rydberg systems.

As expected, the presented results look remarkably similar to those of the diamagnetic

Kepler problem (the quadratic Zeeman effect, see, e.g., Delos *et al* (1983)). The latter can be understood if we note that the Hamiltonian (1) can be rewritten in the form

$$\mathcal{H} = \frac{p^2}{2} - \frac{Q(r)}{r} + c\rho^2, \tag{19}$$

where $Q(r) = 1 + 2cr^3$ (effective charge) and $c = 1/16d^3$. The spherically symmetric part $Q(r)/r$ breaks the Coulomb degeneracy, slightly raising the energies of high l-states. The other term is equivalent to a diamagnetic term. Since we expect ρ^2 to have more effect than r^3, we are not surprised to find that the energies and wavefunctions look very much like those of the diamagnetic Kepler system.

Finally, it should be mentioned that at very large separations, the retardation effects in the interaction (i.e. the effects because of its finite velocity) might, in principle, be significant (see e.g. Margenau and Kestner 1971). However, as it has been noted in the introduction, in this paper we have considered the problem in the approximation of the *instantaneous* van der Waals interaction. This requires that the electron moves so slowly that the interaction can be treated as static, and all retardation effects can be neglected. In this sense, although an exact (QED) analysis would be desirable, simple considerations indicate that this holds for the Rydberg states at the distances presented here.

Acknowledgments

We thank the referees for their useful comments and suggestions. This work has been supported by the Ministry of Science and Technology of Serbia and by the University of La Rioja, project no API-98/B24.

References

Abraham R and Marsden J E 1980 *Foundations of Mechanics* (Reading, MA: Benjamin-Cummings)
Alhassid Y, Hinds E A and Meschede D 1987 *Phys. Rev. Lett.* **59** 1545
Anderson A, Haroche S, Hinds E A, Jhe W and Meschede D 1988 *Phys. Rev.* A **37** 3594
Berry M V 1983 *Proc. Chaotic Behaviour of Deterministic Systems (Les Houches Summer School, Session 36)* ed G R Iooss *et al* (Amsterdam: North-Holland) p 171
Cacciani P, Luc-Koenig E, Pinard J, Thomas C and Liberman S 1986 *Phys. Rev. Lett.* **56** 1467–70
Coffey S L, Deprit A, Miller B R and Williams C A 1986 *Ann. NY Acad. Sci.* **497** 22–36
Delos J B, Knudson S K and Noid D W 1983 *Phys. Rev.* A **28** 7–21
Deprit A 1969 *Celest. Mech.* **1** 12–30
——1981 *Celest. Mech.* **26** 9
Deprit A and Ferrer S 1990 *Rev. Acad. Cienc. Zaragoza* **45** 111–25
Deprit A, Lanchares V, Iñarrea M, Salas J P and Sierra J D 1996 *Phys. Rev.* A **54** 3885–93
Elipe A and Ferrer S 1994 *Phys. Rev. Lett.* **72** 985–8
Fabre C, Gross M, Raimond J M and Haroche S 1983 *J. Phys. B: At. Mol. Phys.* **16** L671–7
Farrelly D and Krantzman K 1991 *Phys. Rev.* A **43** 1666–8
Gallagher T F 1994 *Rydberg Atoms* (*Cambridge Monographs on Atomic and Molecular Physics vol 3*) (Cambridge: Cambridge University Press)
Ganesan K and Lakshmanan M 1992 *Phys. Rev.* A **45** 1548–55
Ganesan K and Taylor K T 1996 *J. Phys. B: At. Mol. Opt. Phys.* **29** 1293–306
Goldstein B 1980 *Classical Mechanics* 2nd edn (Reading, MA: Addison-Wesley)
Lennard-Jones J 1932 *Trans. Faraday Soc.* **28** 333
Margenau H and Kestner N R 1971 *Theory of Intermolecular Forces* 2nd edn (Oxford: Pergamon)
Salas J P, Deprit A, Ferrer S, Lanchares V and Palacián J 1998 *Phys. Lett.* A **242** 83–93
Sandogher V, Sukenik C I, Hinds E A and Haroche S 1992 *Phys. Rev. Lett.* **68** 3432
Simonović N S 1997 *J. Phys. B: At. Mol. Opt. Phys.* **30** L613
Solov'ev E A 1982 *Sov. Phys.–JETP* **55** 1017

Uzer T, Farrelly D, Milligan J Z, Raines P E and Skelton J P 1991 *Science* **242** 42
Waterland R L, Delos J B and Du M L 1987 *Phys. Rev.* A **35** 5064–80
Wintgen D and Friedrich H 1989 *Phys. Rep.* **183** 37–79
Wolfram S 1996 *Mathematica* (New York: Cambridge University Press)
Zaremba E and Kohn W 1976 *Phys. Rev.* B **13** 2270